Screen Printing as a Scalable and Low-Cost Approach for Rigid and Flexible Thin-Film Transistors Using Separated Carbon Nanotubes

Xuan Cao,[†] Haitian Chen,[‡] Xiaofei Gu,[†] Bilu Liu,[‡] Wenli Wang,[‡] Yu Cao,[‡] Fanqi Wu,[†] and Chongwu Zhou*[,†,‡]

[†]Department of Materials Science, University of Southern California, Los Angeles, California 90089, United States and [‡]Department of Electrical Engineering, University of Southern California, Los Angeles, California 90089, United States

ABSTRACT Semiconducting single-wall carbon nanotubes are very promising materials in printed electronics due to their excellent mechanical and electrical property, outstanding printability, and great potential for flexible electronics. Nonetheless, developing scalable and low-cost approaches for manufacturing fully printed high-performance single-wall carbon nanotube thin-film transistors remains a major challenge. Here we report that screen printing, which is a simple, scalable, and cost-effective technique, can be used to produce both rigid and flexible thin-film transistors using separated single-wall carbon nanotubes. Our fully printed top-gated nanotube thin-film transistors on rigid and flexible substrates exhibit decent performance, with mobility up to 7.67 $cm^2 V^{-1} s^{-1}$, on/off ratio of $10^4 \sim 10^5$, minimal hysteresis, and low operation voltage (<10 V). In addition, outstanding mechanical flexibility of printed nanotube thin-film transistors (bent with radius of curvature down to 3 mm) and driving capability for organic light-emitting diode have been demonstrated. Given the high performance of the fully screen-printed single-wall carbon nanotube thin-film transistors, we believe screen printing stands as a low-cost, scalable, and reliable approach to manufacture high-performance nanotube thin-film transistors for application in display electronics. Moreover, this technique may be used to fabricate thin-film transistors based on other materials for large-area flexible macroelectronics, and low-cost display electronics.

KEYWORDS: single-wall carbon nanotube · screen printing · thin-film transistor · flexible electronics · organic light-emitting diode

Printing technology in manufacturing electronics has drawn tremendous interest during the past few decades.[1−12] Compared with traditional fabrication approaches in which multistaged photolithography and vacuum deposition are required, printing is a cost-effective and scalable technology with high throughput and is highly compatible with low-temperature processing, which provides an important way in mass production of large-area flexible electronics at extremely low cost.[13,14] Among various kinds of printed electronics, separated single-wall carbon nanotube (SWCNT) thin-film transistors (TFTs) have attracted growing attention due to their high mobility, high on/off ratio, low operation voltage, and potential application in flexible electronics.[15−19]

Recently, intensive research effort has been devoted to develop low-cost printed SWCNT TFTs and integrated circuits with high performance. The printing techniques used in the past research can be mainly divided into two groups. The first one is of high registration accuracy represented by aerosol−jet printing and inkjet printing. The second one is of high scalability and throughput represented by gravure printing and flexographic printing. Up until now, inkjet and aerosol−jet printing have been used for fabricating SWCNT TFTs,[20−22] 2T1C pixel control circuits for organic light-emitting diode (OLED) control[23] and digital circuit applications.[20,24,25] The advantages of those two printing techniques are the high printing resolution and uniformity,[9] which endow printed devices with small dimension and decent electrical performance. Nevertheless, those techniques, limited by low scalability and throughput, may not be suitable for mass production to further reduce the cost of printed electronics. For research of highly scalable printing

* Address correspondence to chongwuz@usc.edu.

Received for review October 20, 2014 and accepted December 3, 2014.

Published online 10.1021/nn505979j

technology of SWCNT TFTs, pioneer work has been done by Cho's group which demonstrated gravure-printing-based R2R process for manufacturing carbon nanotube (CNT) radio frequency identifications,[26] full adders[27] and D flip-flops.[28] However, the performance is moderate due to the nature of printed layers and the quality of the active channel material.[29] Recently, as a milestone, Javey's and Cho's group reported fully gravure-printed large-area flexible top-gated CNT TFTs with excellent electrical performance.[29] In their work, semiconductor-concentrated nanotube solution was used as channel material and high-k barium titanate (BTO)/poly(methyl methacrylate) hybrid ink was printed as gate dielectric, which significantly improved the mobility (μ) and on/off ratio of the printed SWCNT devices. Moreover, the printed devices showed low operation voltage (<10 V) and outstanding mechanical bendability. Later in 2013, flexographic printing and transfer were reported by Ohno's group for SWCNT TFT fabrication, starting from SWCNTs grown by chemical vapor deposition.[30] Mobility of 157 $cm^2\ V^{-1}\ s^{-1}$ was achieved by using polyimide as the gate dielectric for the back-gated devices.

Screen printing, in which screen masks are used to deposit materials onto large-area substrates with high throughput, is considered as one of the scalable printing techniques and has been widely used in printed electronics.[1,7,31−33] Benefiting from its simplicity, scalability and environment-friendly process,[1,31] this technique shows tremendous potential for mass production of large-area electronics at very low cost. There are two advantages of screen printing when compared with other scalable printing techniques such as gravure or flexographic printing. First, the masks for screen printing are usually made of fabric or stainless steel mesh, which are much more cost-effective than engraved metal masks for gravure printing.[13] The second advantage is that alignment between the screen mask and the substrate can be easily performed right before printing, as the screen mask is semitransparent, and both the screen mask and the substrate are planar. These advantages enables the alignment to be performed in a parallel-plate fashion with good accuracy. In contrast, the gravure printing and flexographic printing usually have either the mask or the substrate on a roller, making alignment in both X and Y direction difficult. Hence, the alignment capability of screen printing makes this technique particularly suitable for fabrication of multilayered structures. A lot of research has been done in screen-printed TFTs, especially for organic TFTs.[32] However, the performance is usually limited by the inherent properties of the organic channel materials.

In this paper, we report the first fully screen-printed top-gated TFTs on rigid and flexible substrates using semiconductor-enriched SWCNT solutions. Silver (Ag) source (S) and drain (D), high-k barium titanate dielectric and Ag gate (G) were printed sequentially in the fabrication process with low-temperature baking (~140 °C). The printed devices showed mobility up to 7.67 $cm^2\ V^{-1}\ s^{-1}$, low operation voltage (<10 V), current on/off ratio of $10^4 \sim 10^5$, and excellent mechanical flexibility. In addition, OLED control capability of printed SWCNT TFTs was demonstrated by connecting an external OLED to a representative TFT. Overall, the good electrical characteristics, low-temperature and cost-effective fabrication process, and outstanding mechanical flexibility of fully printed SWCNT TFTs suggest screen printing is very promising to become a practical technique for device and display applications.

RESULTS AND DISCUSSION

Figure 1a illustrates the fabrication process of printed TFTs on rigid Si/SiO_2 wafer and flexible poly(ethylene terephthalate) (PET) substrate. The surface of substrate was first functionalized with poly-L-lysine and then a uniform random SWCNT network was formed by immersing the substrate into semiconductor-enriched SWCNT solution for 35 min. Second, Ag source, drain, and barium titanate dielectric were printed, followed by etching of unwanted SWCNTs that were not covered by Ag electrodes and BTO dielectric. Finally, Ag gate was printed. More details of the experiments are shown in the Method Section. Figure 1b shows the configuration of a fully printed TFT on PET substrate and Figure 1c is a schematic diagram exemplifying the screen printer and screen printing process. Ink was first applied on the screen mask by a stainless spatula and then spread by a squeegee on the whole patterned area. Then the squeegee was moved across the mask with certain pressure so that the ink was squeezed through the mesh in the desired pattern area and then printed on the substrate. Eventually, the printed layer was cured in an oven at 140 °C. In the printing process, mask specifications, clearance, squeegee angle, printing speed, ink properties, and pressure are key factors which determine the quality of printed layers.[31] In addition, there are *X-Y-θ* adjustment micrometers on the printer to ensure good alignment between different layers. Figure 1d,e shows optical images of printed 12 × 10 TFT arrays on a Si/SiO_2 and a PET substrate, respectively. The SWCNT network was inspected by field-emission scanning electron microscopy (FE-SEM) as shown in Figure 1f.

We carried out significant amount of work to optimize the printed TFT performance by using BTO ink and Ag ink of different concentrations prepared*via* dilution. The characteristics of TFTs printed with different ink dilution ratios are shown in Figure 2. We selected TFTs with channel length (L) ~ 105 μm and channel width (W) ~ 1000 μm as examples. BTO and Ag inks were purchased from commercial sources and then diluted using diethylene glycol ethyl ether acetate as the solvent with different volume ratio (V_{sol}/V_{ink}).

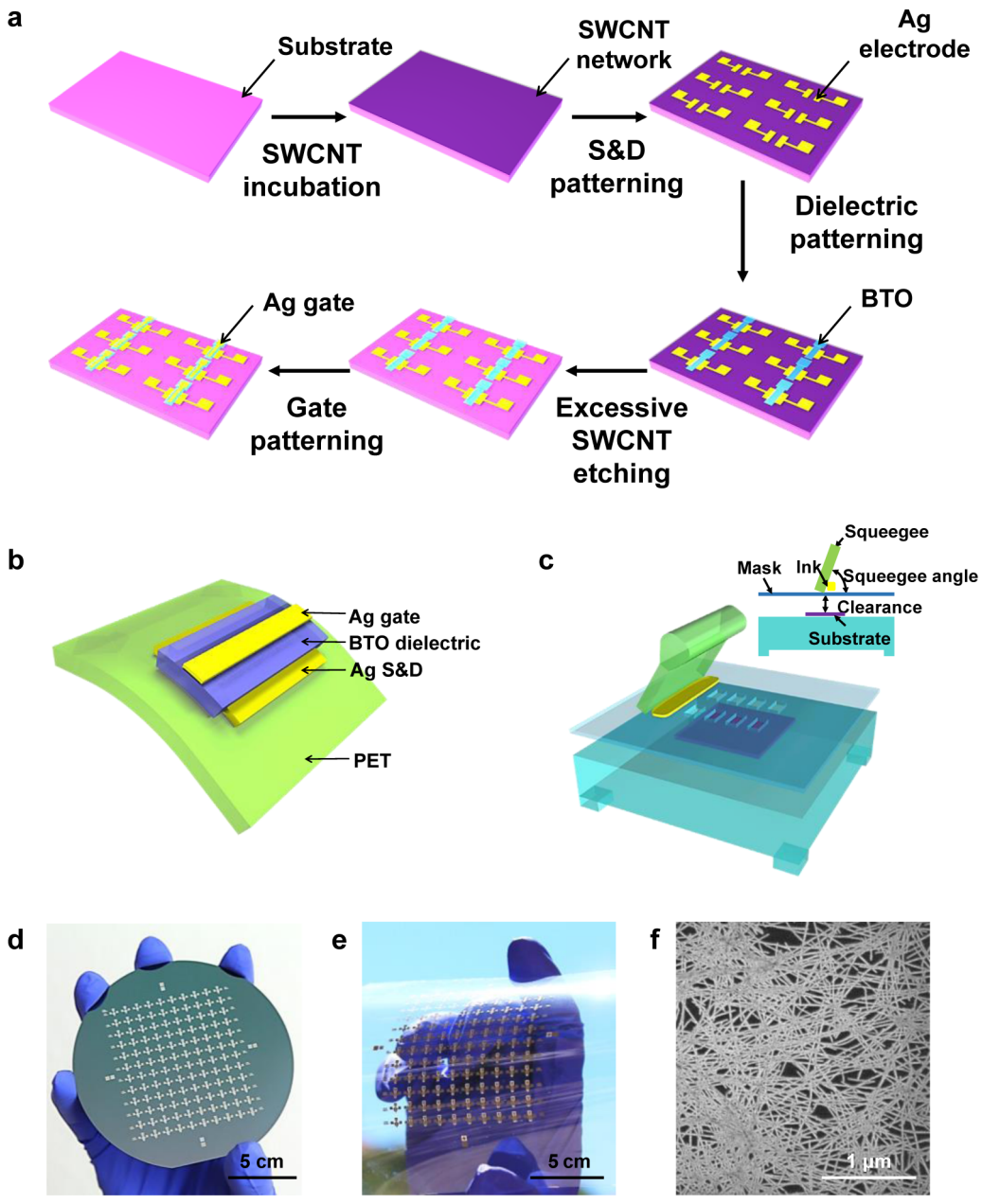

Figure 1. Fully screen-printed SWCNT TFTs on rigid and flexible substrates. (a) Schematic diagram shows the fabrication process of fully printed top-gated SWCNT TFTs. (b and c) Schematic diagrams show the configuration of a fully printed TFT on PET substrate and screen printing system, respectively. (d and e) Optical images of fully printed TFT arrays on a 4 in. Si/SiO_2 wafer (d) and a 12 × 12 cm PET sheet (e). (f) FE-SEM image of deposited SWCNT film.

Figure 2a,b shows the thickness variation of printed BTO and Ag layers as a function of V_{sol}/V_{ink}. Due to the nature of screen printing, ink used for this technique requires high viscosity, which results in inherently thick printed layers. In Figure 2a,b, the thicknesses of undiluted (UD) BTO and Ag layers after printing are 8.1 and 10 μm, respectively, measured using a profilometer. The thickness variation from sample to sample was observed to be around $\pm$0.5 μm. We note the thickness can be reduced by diluting the inks. For example, diluted BTO ink with V_{sol}/V_{ink} = 1:4 led to printed BTO layer of ~5 μm in thickness, while diluted Ag ink with V_{sol}/V_{ink} = 1:4 and V_{sol}/V_{ink} = 1:3 led to Ag electrode of ~6 μm and ~3.5 μm, respectively. To facilitate printing of multiple layers for the SWCNT TFTs, we needed Ag source and drain electrodes with height that would not negatively affect the printing of subsequent BTO, so we focused on Ag inks diluted with volume ratios of 1:4 and 1:3. The transfer characteristics of SWCNT TFTs printed using inks of different dilution ratios are shown in Figure 2c,d. To study the effect of BTO ink dilution, we can first compare the curves in Figure 2c,d corresponding to diluted Ag ink with V_{sol}/V_{ink} = 1:3. When undiluted BTO ink was used, the printed SWCNT TFTs show low on-current (~0.4 μA) and low transconductance (~0.059 μS/mm)

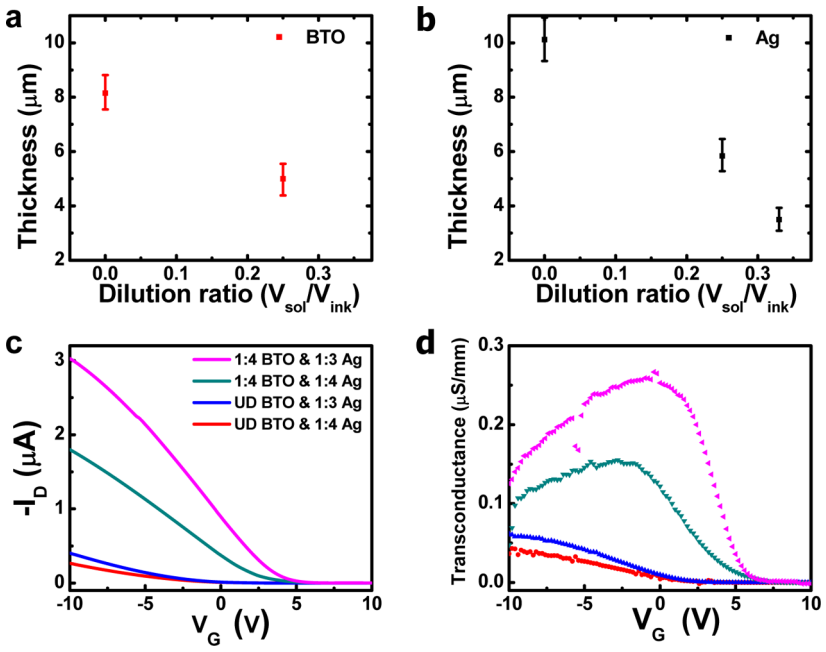

Figure 2. Characterization of SWCNT TFTs printed with different ink dilution conditions. (a and b) Thicknesses of printed BTO and silver layers as a function of dilution ratios. (c) Transfer (I_D-V_G) characteristics of TFTs printed with inks of different dilution ratios (V_{sol}/V_{ink}), measured at $V_{DS} = -1$ V. (d) Transconductance exacted as a function of gate voltage.

at $V_G = -10$ V and $V_{DS} = -1$ V. Remarkably, on-current and the peak of transconductance (Figure 2d) increased up to ~3 μA and ~0.27 μS/mm when we used the 1:4 diluted BTO for dielectric layer. We attribute the improved on-current to both improvement in gate capacitance and mobility when thinned dielectric was used. First of all, at a given gate voltage (V_G), thinner gate dielectric can lead to higher gate capacitance and stronger gate-channel coupling, and thus the number of carriers in the channel increases. Moreover, based on the multiple trap and release (MTR) model,[33] the increased charge in the channel can lead to greater filling of interface traps, causing the ratio of free to trapped carriers to increase. As a result, devices with thinner dielectrics would show higher field-effect mobility. Both the enhanced mobility and increased number of carriers contributed to larger drain current (I_D) and transconductance when diluted BTO was used.

In addition, we observed that Ag inks of different dilution ratios also affect the performance of printed devices even when the same kind of BTO was used for gate dielectric printing. As shown in Figure 2c,d, with the same dilution ratio of BTO, more diluted Ag ink for source and drain would improve the on-current and peak transconductance. Interestingly, we found that dilution of Ag ink for source and drain had an important effect on the thickness of the subsequent printed BTO dielectric, which had a direct impact on the device performance. Here we propose that capillary effect plays a critical role in the solution-based printing process. After source and drain printing, a "trench" with width = 105 μm in the channel region was formed between the rather high source and drain electrodes. A deeper trench formed by less-diluted Ag source and drain would have stronger capillary effect and thus more BTO material would be trapped in the trench when BTO was printed. Hence, the resulted printed BTO was thicker than the BTO layer in more-diluted S/D case. As shown in Supporting Information Figure S1, with the same BTO ink with V_{sol}/V_{ink} = 1:4 for dielectric, the resulted BTO layer when 1:3 diluted Ag ink was used for source and drain is ~5 μm in thickness and thinner than the ~6.5 μm BTO layer when 1:4 diluted Ag ink was used for source and drain patterning. Nonetheless, overdiluted BTO (V_{sol}/V_{ink} > 1:4) caused gate leakage through pinholes in the gate dielectric. Hence we optimized the ink dilution as V_{sol}/V_{ink} = 1:3 for Ag source and drain, V_{sol}/V_{ink} = 1:4 for BTO gate dielectric, and undiluted Ag ink for gate for the following study, and the profiles of the printed electrode, dielectric layer, and gate are shown in Supporting Information Figure S2 as examples.

On the basis of the optimized dilution conditions, the electrical performance of fully printed SWCNT TFTs on rigid Si/SiO_2 substrate was further studied, as shown in Figure 3. Transfer characteristics of a representative TFT with $L = 105$ μm and $W = 1000$ μm are shown in Figure 3a. The device exhibits current on/off ratio of ~3×10^4, extremely small hysteresis, and normalized peak transconductance of ~0.43 μS/mm at $V_{DS} = -1$ V. The mobility was calculated with the following equation:[23]

$$\mu = \frac{L}{W}\frac{1}{C_{ox}V_{SD}}\frac{dI_{SD}}{dV_G}$$

where L and W are the channel length and width of the device. V_{SD} is the source and drain voltage and

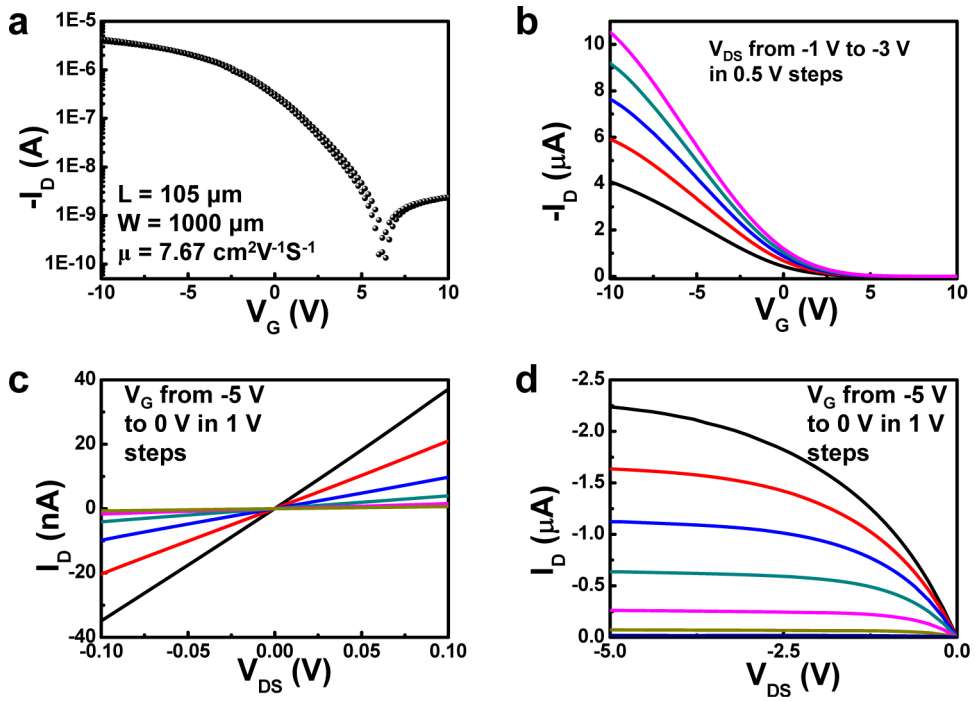

Figure 3. Electrical characteristics of fully printed top-gated SWCNT TFTs on Si/SiO_2 substrate, with ink dilution of V_{sol}/V_{ink} = 1:3 for the silver source and drain, V_{sol}/V_{ink} = 1:4 for the BTO dielectric, and undiluted silver for the gate. (a) Double-sweep of transfer characteristics of a representative TFT measured at $V_{DS} = -1$ V, showing very small hysteresis. (b) Transfer characteristics under different drain voltages (from −1 to −3 V in 0.5 V steps). (c and d) Output characteristics of the same device in triode regime (c) and saturation regime (d), respectively.

is 1 V. I_{SD} is the current flowing from source to drain and V_G is the gate voltage. C_{ox} is the gate capacitance per unit area and can be calculate using the following equation if we consider the SWCNT network as a uniform thin-film:[23]

$$C_{ox} = \frac{\varepsilon_0 \varepsilon_r}{t_{ox}} = 6.195 \times 10^{-9}\ \mathrm{F/cm^2}$$

where ε_r is the relative dielectric constant of the BTO (∼35 for the BTO ink we used), ε_0 is the vacuum dielectric constant, and t_{ox} is the thickness of the BTO layer (∼5 μm). Then the calculated field effect mobility is 7.67 cm^2V^{-1} S^{1-}. The gate leakage current as a function of gate voltage at $V_{DS} = -1$ V is shown in Supporting Information Figure S3, and the small leakage current (<0.5 nA) indicates excellent insulating property of the printed BTO dielectric layer. The transfer curves with V_{DS} ranging from −0.1 to 0.1 V are shown in Figure 3b. The output curves in Figure 3c exhibits a clear linear regime, illustrating good ohmic contacts between the printed Ag electrode and the SWCNT network. Additionally, current saturation due to pinch-off effect was clearly observed as shown in Figure 3d. Statistical study of 15 fully screen printed SWCNT TFTs with L ∼ 105 μm and W ∼ 1000 μm is shown in Supporting Information Figure S4, exhibiting good uniformity in terms of mobility, current on/off ratio, on-current density, and threshold voltage.

After the demonstration of fully printed high-performance SWCNT TFTs on rigid substrate, screen printing was also used in fabricating SWCNT TFTs on flexible substrate. Figure 4 shows the mechanical flexibility of fully screen-printed TFTs on PET substrate. Flexible TFTs were wrapped onto glass vials of different radii (R) during the measurement. The optical image of the measurement setup is shown in Figure 4a and the transfer characteristics of different bending conditions are shown in Figure 4b. The extracted mobility and on/off ratio as a function of bending radius in Figure 4c,d indicate that there is little measurable degradation of the flexible SWCNT TFT while bent with radius of curvature down to 3 mm. Our results indicate the great mechanical stability and flexibility of the SWCNT network and the TFT structure.

On the basis of the measured high on/off ratio, high mobility, small hysteresis, and low operation voltage, we further studied the application of these fully printed low-cost SWCNT TFTs in display electronics. For proof of concept, a typical printed top-gated TFT was connected to an external OLED, whose structure is shown in Supporting Information Figure S5. The schematic diagrams of the measured circuits are in the insets of Figure 5a−c. The current which flows through the OLED (I_{OLED}) is plotted as a function of gate voltage at different V_{DD} in Figure 5a. A driving current of 22.5 μA was measured at $V_G = -20$ V and $V_{DD} = 5$ V, which is more than sufficient for driving the OLED that requires 1 μA to have observable light emission. The family curves of $I_{OLED} - V_{ss}$ measured at different gate voltages are shown in Figure 5b, and Figure 5c

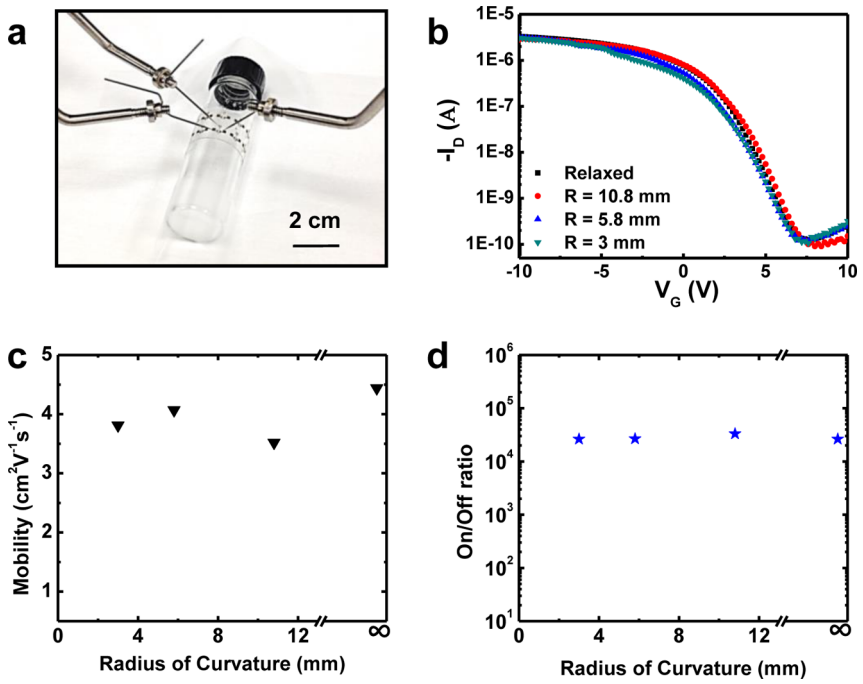

Figure 4. Mechanical flexibility of fully printed flexible SWCNT TFTs on PET substrate, with ink dilution of V_{sol}/V_{ink} = 1:3 for the silver source and drain, $V_{sol}V_{ink}$ = 1:4 for the BTO dielectric, and undiluted silver ink for the gate. (a) Optical image of electrical measurements on a printed TFT while bent. (b) Transfer (I_D-V_G) characteristics of a representative device under different bending conditions of relaxed and bent at different radii of curvature (R), measured at $V_{DS} = -1$ V. (c) Field-effect mobility and (d) I_{on}/I_{off} plotted as a function of bending radius of curvature (R) of relaxed state is infinite).

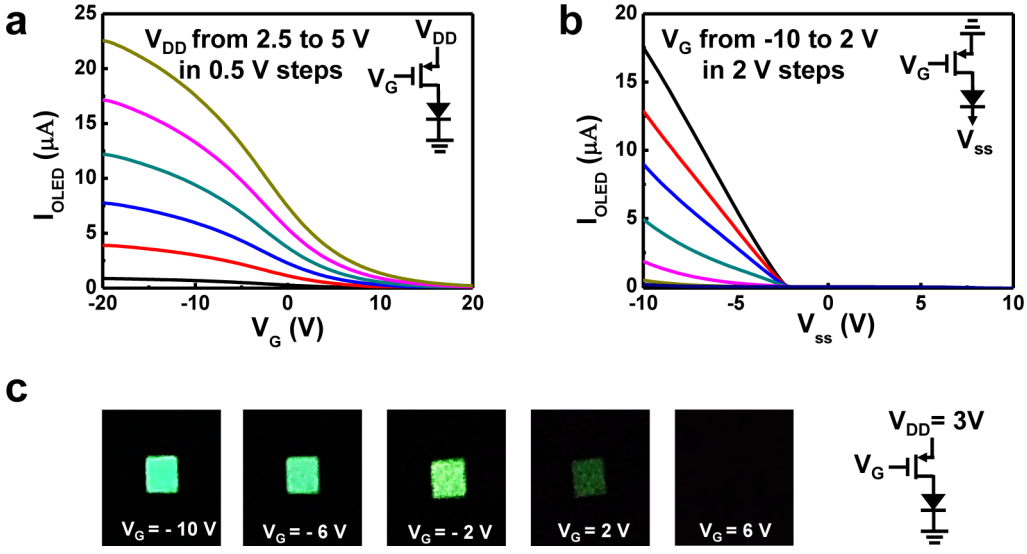

Figure 5. Fully printed SWCNT TFTs for OLED control. (a) $I_{OLED}-V_G$ family curves correspond to values of V_{DD} from 2.5 to 5 V in 0.5 V steps. (b) $I_{OLED}-V_{SS}$ family curves correspond to values of V_G from −10 to 2 V in 2 V steps. (c) Optical images showing external OLED intensity change *versus* V_G with V_{DD} = 3 V.

indicates that the intensity of light emission changed with increasing V_G. The OLED was very bright at V_G = −10 V, V_{DD} = 3 V and then the light intensity was reduced by increasing V_G. Eventually, the OLED was turned off at V_G = 6 V. On the basis of the data above, we demonstrated that the fully screen-printed SWCNT TFTs exhibited good OLED control capability and might have potential for large-area, flexible and low-cost display electronics applications.

CONCLUSION

In summary, we have fabricated fully screen-printed top-gated SWCNT TFTs on both rigid and flexible substrates. In this study, semiconductor-enriched SWCNT solution was used as channel materials and high-k gate dielectric was printed. In addition, the optimization of ink dilution was studied and the printed devices exhibited mobility up to 7.67 $cm^2 V^{-1} s^{-1}$, on/off ratio of $10^4 \sim 10^5$,

minimal hysteresis, low operation voltage, and outstanding mechanical flexibility. On the basis of the good performance, the OLED driving capability of fully printed TFTs was demonstrated. Our work shows that screen printing has great potential for mass production of large-area, cost-effective and high-performance CNT TFTs for applications in macroelectronic applications.

One concern about screen printing may be the printing resolution, which is related to several factors. First of all, specifications of the screen mask is an important factor including the mechanical strength of the metal mesh, emulsion thickness, wire diameter, and opening ratio. Recently, 6 μm resolution screen printing has been reported by improving the quality of the screen masks.[34] Second, ink and substrate also affect the printing resolution. Most of the inks used for screen printing are composed of nanoparticles, binders, and solvents. The diameter of the nanoparticles and affinity of the ink to the substrate play significant roles influencing the printing resolution. Overall, screen printing holds great promise for high-resolution printing in the future.

METHODS

Separated Nanotube Deposition. The substrates of Si/SiO_2 (oxide ~300 nm) or PET (~200 μm, Asada mesh, Inc.) were first cleaned with oxygen plasma under 100 W for 90 s.Then the substrates were immersed in poly-L-lysine aqueous solution (0.1% w/v, TED PELLA, Inc.) for 8 min to functionalize the surface. This step was followed by rinsing the functionalized substrate using deionized (DI) water. Later, SWCNT network was deposited by immersing the substrate in purified semiconductor-enriched CNT solution (IsoSol-S100, #23−081, Nanointegris, Inc.) for 35 min. After rinsed with DI water and dried by nitrogen gun, the samples were baked on a hot plate at 120 °C for 1 h. Unwanted SWCNTs were etched using oxygen plasma (100 W) for 80s.

Ink Dilution and Screen Printing. In this work, both the silver ink (AG-959, Conductive Compounds Inc.) and BTO ink (BT-101, Conductive Compounds, Inc.) were diluted by diethylene glycol ethyl ether acetate (Solvent 20, Conductive Compounds, Inc.). Thicknesses of printed layers were measured by a profilometer (Dectak II, Veeco). During printing, the screen printer (ZT-320, TOPRO Ltd.) was manually operated with squeegee angle (see Figure 1c) of 80° and clearance of 1.25 mm for silver ink and 1.5 mm for BTO ink, at a printing speed ~30 cm/s. After printing, samples were baked in an oven (Blue M 0 V-8A) at 140 °C for 2 min (for silver electrode) or 8 min (for BTO dielectric). Electrical measurements were carried out using an Agilent 4156B under ambient conditions.

Conflict of Interest: The authors declare no competing financial interest.

Acknowledgment. We would like to acknowledge the collaboration of this research with King Abdul-Aziz City for Science and Technology (KACST) *via* The Center of Excellence for Green Nanotechnologies (CEGN).

Supporting Information Available: Additional SEM images, profilometer results, device characteristics, statistical study of printed SWCNT TFTs, and schematics of the OLED structure. This material is available free of charge via the Internet at http://pubs.acs.org.

REFERENCES AND NOTES

1. Bao, Z. N.; Feng, Y.; Dodabalapur, A.; Raju, V. R.; Lovinger, A. J. High-Performance Plastic Transistors Fabricated by Printing Techniques. *Chem. Mater.* **1997**, *9*, 1299–1301.
2. Berggren, M.; Nilsson, D.; Robinson, N. D. Organic Materials for Printed Electronics. *Nat. Mater.* **2007**, *6*, 3–5.
3. Cho, J. H.; Lee, J.; Xia, Y.; Kim, B.; He, Y. Y.; Renn, M. J.; Lodge, T. P.; Frisbie, C. D. Printable Ion-Gel Gate Dielectrics for Low-Voltage Polymer Thin-Film Transistors on Plastic. *Nat. Mater.* **2008**, *7*, 900–906.
4. Li, Y. N.; Wu, Y. L.; Ong, B. S. Facile Synthesis of Silver Nanoparticles Useful for Fabrication of High-Conductivity Elements for Printed Electronics. *J. Am. Chem. Soc.* **2005**, *127*, 3266–3267.
5. Minemawari, H.; Yamada, T.; Matsui, H.; Tsutsumi, J.; Haas, S.; Chiba, R.; Kumai, R.; Hasegawa, T. Inkjet Printing of Single-Crystal Films. *Nature* **2011**, *475*, 364–367.
6. Park, J. U.; Hardy, M.; Kang, S. J.; Barton, K.; Adair, K.; Mukhopadhyay, D. K.; Lee, C. Y.; Strano, M. S.; Alleyne, A. G.; Georgiadis, J. G.; *et al.* High-Resolution Electrohydrodynamic Jet Printing. *Nat. Mater.* **2007**, *6*, 782–789.
7. Sekitani, T.; Nakajima, H.; Maeda, H.; Fukushima, T.; Aida, T.; Hata, K.; Someya, T. Stretchable Active-Matrix Organic Light-Emitting Diode Display Using Printable Elastic Conductors. *Nat. Mater.* **2009**, *8*, 494–499.
8. Sekitani, T.; Takamiya, M.; Noguchi, Y.; Nakano, S.; Kato, Y.; Sakurai, T.; Someya, T. A Large-Area Wireless Power-Transmission Sheet Using Printed Organic Transistors and Plastic Mems Switches. *Nat. Mater.* **2007**, *6*, 413–417.
9. Singh, M.; Haverinen, H. M.; Dhagat, P.; Jabbour, G. E. Inkjet Printing-Process and Its Applications. *Adv. Mater.* **2010**, *22*, 673–685.
10. Willmann, J.; Stocker, D.; Dorsam, E. Characteristics and Evaluation Criteria of Substrate-Based Manufacturing. Is Roll-to-Roll the Best Solution for Printed Electronics? *Org. Electron.* **2014**, *15*, 1631–1640.
11. Yan, H.; Chen, Z. H.; Zheng, Y.; Newman, C.; Quinn, J. R.; Dotz, F.; Kastler, M.; Facchetti, A. A High-Mobility Electron-Transporting Polymer for Printed Transistors. *Nature* **2009**, *457*, 679–686.
12. Fukuda, K.; Takeda, Y.; Yoshimura, Y.; Shiwaku, R.; Tran, L. T.; Sekine, T.; Mizukami, M.; Kumaki, D.; Tokito, S. Fully-Printed High-Performance Organic Thin-Film Transistors and Circuitry on One-Micron-Thick Polymer Films. *Nat. Commun.* **2014**, 10.1038/ncomms5147.
13. Aleeva, Y.; Pignataro, B. Recent Advances in Upscalable Wet Methods and Ink Formulations for Printed Electronics. *J. Mater. Chem. C* **2014**, *2*, 6436–6453.
14. Sun, D. M.; Liu, C.; Ren, W. C.; Cheng, H. M. A Review of Carbon Nanotube- and Graphene-Based Flexible Thin-Film Transistors. *Small* **2013**, *9*, 1188–1205.
15. Sun, D. M.; Timmermans, M. Y.; Tian, Y.; Nasibulin, A. G.; Kauppinen, E. I.; Kishimoto, S.; Mizutani, T.; Ohno, Y. Flexible High-Performance Carbon Nanotube Integrated Circuits. *Nat. Nanotechnol.* **2011**, *6*, 156–161.
16. Wang, C.; Takei, K.; Takahashi, T.; Javey, A. Carbon Nanotube Electronics - Moving Forward. *Chem. Soc. Rev.* **2013**, *42*, 2592–2609.
17. Wang, C.; Zhang, J. L.; Ryu, K. M.; Badmaev, A.; De Arco, L. G.; Zhou, C. W. Wafer-Scale Fabrication of Separated Carbon Nanotube Thin-Film Transistors for Display Applications. *Nano Lett.* **2009**, *9*, 4285–4291.
18. Cao, Q.; Kim, H. S.; Pimparkar, N.; Kulkarni, J. P.; Wang, C. J.; Shim, M.; Roy, K.; Alam, M. A.; Rogers, J. A. Medium-Scale Carbon Nanotube Thin-Film Integrated Circuits on Flexible Plastic Substrates. *Nature* **2008**, *454*, 495–500.
19. Zhang, J. L.; Wang, C.; Zhou, C. W. Rigid/Flexible Transparent Electronics Based on Separated Carbon Nanotube Thin-Film Transistors and Their Application in Display Electronics. *ACS Nano* **2012**, *6*, 7412–7419.

20. Ha, M. J.; Xia, Y.; Green, A. A.; Zhang, W.; Renn, M. J.; Kim, C. H.; Hersam, M. C.; Frisbie, C. D. Printed, Sub-3v Digital Circuits on Plastic from Aqueous Carbon Nanotube Inks. *ACS Nano* **2010**, *4*, 4388–4395.
21. Okimoto, H.; Takenobu, T.; Yanagi, K.; Miyata, Y.; Shimotani, H.; Kataura, H.; Iwasa, Y. Tunable Carbon Nanotube Thin-Film Transistors Produced Exclusively *via* Inkjet Printing. *Adv. Mater.* **2010**, *22*, 3981–3986.
22. Xu, W.; Zhao, J.; Qian, L.; Han, X.; Wu, L.; Wu, W.; Song, M.; Zhou, L.; Su, W.; Wang, C.; Nie, S.; Cui, Z. Sorting of Large-Diameter Semiconducting Carbon Nanotube and Printed Flexible Driving Circuit for Organic Light Emitting Diode (Oled). *Nanoscale* **2014**, *6*, 1589–1595.
23. Chen, P. C.; Fu, Y.; Aminirad, R.; Wang, C.; Zhang, J. L.; Wang, K.; Galatsis, K.; Zhou, C. W. Fully Printed Separated Carbon Nanotube Thin Film Transistor Circuits and Its Application in Organic Light Emitting Diode Control. *Nano Lett.* **2011**, *11*, 5301–5308.
24. Ha, M. J.; Seo, J. W. T.; Prabhumirashi, P. L.; Zhang, W.; Geier, M. L.; Renn, M. J.; Kim, C. H.; Hersam, M. C.; Frisbie, C. D. Aerosol Jet Printed, Low Voltage, Electrolyte Gated Carbon Nanotube Ring Oscillators with Sub-5 μs Stage Delays. *Nano Lett.* **2013**, *13*, 954–960.
25. Kim, B.; Jang, S.; Geier, M. L.; Prabhumirashi, P. L.; Hersam, M. C.; Dodabalapur, A. High-Speed, Inkjet-Printed Carbon Nanotube/Zinc Tin Oxide Hybrid Complementary Ring Oscillators. *Nano Lett.* **2014**, *14*, 3683–3687.
26. Jung, M.; Kim, J.; Noh, J.; Lim, N.; Lim, C.; Lee, G.; Kim, J.; Kang, H.; Jung, K.; Leonard, A. D.; *et al.* All-Printed and Roll-to-Roll-Printable 13.56-MHz-Operated 1-Bit Rf Tag on Plastic Foils. *Ieee. T. Electron Devices* **2010**, *57*, 571–580.
27. Noh, J.; Jung, K.; Kim, J.; Kim, S.; Cho, S.; Cho, G. Fully Gravure-Printed Flexible Full Adder Using Swnt-Based Tfts. *IEEE Electron Device Lett.* **2012**, *33*, 1574–1576.
28. Noh, J.; Jung, M.; Jung, K.; Lee, G.; Kim, J.; Lim, S.; Kim, D.; Choi, Y.; Kim, Y.; Subramanian, V.; *et al.* Fully Gravure-Printed D Flip-Flop on Plastic Foils Using Single-Walled Carbon-Nanotube-Based Tfts. *IEEE Electron Device Lett.* **2011**, *32*, 638–640.
29. Lau, P. H.; Takei, K.; Wang, C.; Ju, Y.; Kim, J.; Yu, Z.; Takahashi, T.; Cho, G.; Javey, A. Fully Printed, High Performance Carbon Nanotube Thin-Film Transistors on Flexible Substrates. *Nano Lett.* **2013**, *13*, 3864–3869.
30. Higuchi, K.; Kishimoto, S.; Nakajima, Y.; Tomura, T.; Takesue, M.; Hata, K.; Kauppinen, E. I.; Ohno, Y. High-Mobility, Flexible Carbon Nanotube Thin-Film Transistors Fabricated by Transfer and High-Speed Flexographic Printing Techniques. *Appl. Phys. Express* **2013**, *6*, 085101.
31. Menard, E.; Meitl, M. A.; Sun, Y. G.; Park, J. U.; Shir, D. J. L.; Nam, Y. S.; Jeon, S.; Rogers, J. A. Micro- and Nanopatterning Techniques for Organic Electronic and Optoelectronic Systems. *Chem. Rev.* **2007**, *107*, 1117–1160.
32. Ryu, G. S.; Kim, J. S.; Jeong, S. H.; Song, C. K. A Printed Otft-Backplane for Amoled Display. *Org. Electron.* **2013**, *14*, 1218–1224.
33. Singh, V. K.; Mazhari, B. Impact of Scaling of Dielectric Thickness on Mobility in Top-Contact Pentacene Organic Thin Film Transistors. *J. Appl. Phys.* **2012**, *111*, 034905.
34. Kuroda Electric Home Page: Http://www.kuroda-electric.eu/Ultra-Fine-Pattern-Screen-Printing.